Geophysical Research Letters

RESEARCH LETTER
10.1029/2022GL099442

Key Points:

- Tropical cyclones that intensify tend to have greater longwave convergence within the atmospheric column prior to intensification
- An operational forecast model can capture the signal of TC intensification in longwave radiation
- The ability to simulate radiation in the forecast model can influence its prediction skills of tropical cyclone intensification

Supporting Information:

Supporting Information may be found in the online version of this article.

Correspondence to:

S.-N. Wu,
swu@ou.edu

Citation:

Wu, S.-N., Soden, B. J., & Alaka, G. J. Jr. (2023). The influence of radiation on the prediction of tropical cyclone intensification in a forecast model. *Geophysical Research Letters*, *50*, e2022GL099442. https://doi.org/10.1029/2022GL099442

Received 2 JUL 2022
Accepted 6 JAN 2023

The Influence of Radiation on the Prediction of Tropical Cyclone Intensification in a Forecast Model

S.-N. Wu[1,2], B. J. Soden[2], and G. J. Alaka Jr.[3]

[1]School of Meteorology, University of Oklahoma, Norman, OK, USA, [2]Rosenstiel School of Marine and Atmospheric Science, University of Miami, Miami, FL, USA, [3]NOAA/AOML/Hurricane Research Division, Miami, FL, USA

Abstract This study examines the influence of radiative heating on the prediction of tropical cyclone (TC) intensification in the Hurricane Weather Research and Forecasting (HWRF) model. Previous idealized modeling and observational studies demonstrated that radiative heating can substantially modulate the evolution of TC intensity. However, the relevance of this process under realistic conditions remains unclear. Here, we use observed longwave radiative heating to explore the performance of TC forecasts in HWRF simulations. The performance of TC intensity forecasts is then investigated in the context of radiative heating forecasts. In observations and HWRF forecasts, high clouds near the TC center increase the convergence of radiative fluxes. A sharp spatial gradient (≥60 W/m^2) in the flux convergence from the TC center outward toward the environment is associated with subsequent TC intensification. More accurate simulation of the spatial structure of longwave radiative heating is associated with more accurate TC intensity forecasts.

Plain Language Summary Satellite measurements observed larger radiation heating near the center of intensifying tropical cyclones. Previous idealized modeling studies suggest that this heating facilitates tropical cyclone development. In this study, we investigate how radiative heating affects the ability of a tropical cyclone forecast model to predict tropical cyclone intensification. Our results demonstrate that the model forecasts of intensity improve when the model better reproduces the observed spatial structure of radiative heating associated with the tropical cyclone.

1. Introduction

The prediction of tropical cyclones (TCs) has been steadily improved over the past two decades (DeMaria et al., 2014; Simon et al., 2018). Increased computational resources have permitted high-resolution simulations to better resolve convective-scale dynamical processes. Improved representation of microphysical and boundary layer processes and refined physical parameterizations in numerical models have also advanced the performance of hurricane forecasting models (Lewis et al., 2020; Mehra et al., 2018; Wang et al., 2018). Despite these advances, significant room for the improvement in TC intensity forecasts remains, especially for rapid intensification events. Moreover, the role of radiative processes in the intensity forecasts has received less attention in operational models, despite a growing number of studies that have demonstrated its importance on TC genesis and intensification (Carstens & Wing, 2020; Muller & Romps, 2018; Smith et al., 2020; Wing et al., 2016; Wu, Soden, Miyamoto et al., 2021; Wu, Soden, Nolen 2021; Zhang, Sieron, et al., 2021; Zhang, Soden, et al., 2021).

Radiation is a critical modulator for atmospheric energy balance and is essential for determining the strength of the global circulation (Fermepin & Bony, 2014; Randall et al., 1989; Sherwood et al., 1994). In addition to their known importance to climate, there is a growing recognition that interactions between clouds and radiation also play a critical role in regulating the intensity of individual high-impact weather systems (Bretherton et al., 2005; Muller & Held, 2012; Wing & Emanuel, 2014; Wing et al., 2016). By enhancing the spatial contrast in atmospheric longwave radiative heating, cloud differences induce a secondary overturning circulation which further intensifies the cloud and precipitation fields.

Recent modeling studies have demonstrated the importance of radiative processes on TC development, particularly at the early stages of development where radiative heating makes up a larger fraction of the total diabatic heating within a storm. In model simulations, suppressing radiative interactions acts to slow or inhibit tropical cyclogenesis, highlighting the potential importance of radiative heating on TC development (Bretherton et al., 2005; Bu et al., 2014; Carstens & Wing, 2020; Fovell et al., 2016; Melhauser & Zhang, 2014; Muller & Romps, 2018; Smith et al., 2020; Wing et al., 2016; Zhang, Soden, et al., 2021; Zhang, Sieron, et al., 2021).

Also, the modification in radiative forcing in full-physics numerical simulations influences the evolution of TC wind fields (Fovell et al., 2016; Melhauser & Zhang, 2014). Modeling studies have also found that the spatial contrast in radiative heating between the TC center and large-scale environment induces a secondary circulation that provides an upgradient transport of moist static energy and accelerates TC development (Carstens & Wing, 2020; Smith et al., 2020; Wu, Soden, Miyamoto et al., 2021; Wu, Soden, Nolen 2021). These findings suggest that the accuracy of TC intensity forecasts produced by numerical models may also depend, in part, on the accurate simulation of the spatial distribution of radiative heating in the TC area relative to its surroundings.

Imposing external forcings on TCs in numerical simulations can also enhance the predictability of TC intensity. Significant large-scale environmental influences such as strong vertical wind shear can elevate the predictability, increasing the accuracy of the forecasted TC evolution (Finocchio & Majumdar, 2017; Zhang & Tao, 2013). Without large-scale environmental influences, the intensity forecasting error in numerical simulations will grow faster, because the effectiveness of the intrinsic predictability associated TC internal dynamics sharply diminished within 3 days (Hakim, 2013; Judt & Chen, 2016) Therefore, correctly reproducing the observed radiative heating, which is an important large-scale forcing for weaker TCs (e.g., Wing et al., 2016), could enhance the predictability of TC intensity by lowering the growth rate of errors.

This study aims to expand our understanding of the relationship between radiative heating and TC evolution to a more practical approach. We compare the observed spatial distribution of radiative heating in Hurricane Weather and Research Forecasting (HWRF) model simulations with that from satellite observations. The performance of radiative heating forecasts in HWRF is further examined based on different forecast skills of TC intensity. We use the NASA Clouds and the Earth's Radiant Energy System (CERES) measurements to quantify the relationship between observed atmospheric longwave radiative heating and subsequent TC intensity change. It is shown that, in both observations and HWRF simulations, storms with large radiative heating tend to show a larger subsequent increase in TC intensity. Simulated storms with a spatial distribution of longwave heating similar to that observed tend to have a better prediction of the subsequent 24-hr intensification change.

2. Data and Methods

2.1. CERES Measurements

The CERES instruments mounted on the Terra and Aqua satellites provide a radiative energy budget at the top of the atmosphere across the globe (Fueglistaler, 2019; Loeb et al., 2020; Wielicki et al., 1996). In this study, we use the "synoptic TOA and surface fluxes and clouds" data set (SYN1deg-1Hour; Doelling et al., 2013), which provides radiative fluxes at the top-of-atmosphere and the surface, with a horizontal latitude/longitude grid spacing of one degree and a time interval of 1 hour. The radiative fluxes in SYN1deg-1Hour were retrieved using the CERES measurements in combination with longwave observations and cloud properties from geostationary satellites. In this study, we use CERES radiative flux measurements in the 2018 North Atlantic and eastern North Pacific hurricane seasons, co-locating these data in space/time with simulated TCs and then comparing them with HWRF radiative flux forecasts.

2.2. TC Intensity and Location

International Best Track Archive for Climate Stewardship (IBTrACS) offers 6-hourly maximum wind speed and location of historical TCs (Knapp et al., 2010). The resolution of the intensity is 5 kt and location is rounded to the nearest tenth of a degree. IBTrACS is used to locate TCs in CERES measurements and to identify TC intensity at the analysis time and 24 hr later. The 24-hr intensity change in this study is defined as the difference between the current intensity and the intensity 24 hr later. The reason for choosing 24-hr interval is motivated by the response time for the overturning circulation, which takes approximately one day to reach the TC core from the environment. If TC intensity increases at least by 5 kt, it is classified as an intensifying TC. Conversely, if TC intensity decreases by at least 5 kts over the subsequent 24 hr, it is classified as a weakening TC. To minimize the influence of current TC intensity on the signal of TC intensification (Wu & Soden, 2017; Wu, Soden, Miyamoto, et al., 2021; Wu, Soden, Nolen, 2021; Wu et al., 2020), we stratify these TCs based on their TC intensity at the analysis time: tropical depression (TD; <34 kt), tropical storm (TS; 34–63 kt), Category 1–2 TC (Cat 1–2; 64–112 kt), and Category 3–5 TC (Cat 3–5; >112 kt).

2.3. HWRF Simulations

The HWRF (Atlas et al., 2015; Bao et al., 2012; Gopalakrishnan et al., 2011, 2012, 2013; Mehra et al., 2018; Tallapragada et al., 2014) is one of the top-performing operational hurricane prediction models (Lewis et al., 2020). HWRF was developed for operational use at the National Oceanic and Atmospheric Administration in 2007 with support from the Hurricane Forecast Improvement Project (HFIP; Gall et al., 2013; Gopalakrishnan et al., 2021). Storm-following nested domains are a premier component of HWRF that have improved forecasts, in particular, intensity forecasts, dramatically over the last decade (Alaka et al., 2022; Gopalakrishnan et al., 2021). HWRF is configured with two telescopic, nested domains (grid spacings of 4.5 and 1.5 km, respectively) that follow a TC to produce high-resolution forecasts within a larger outermost domain that captures the synoptic-scale environment at 13.5-km resolution. HWRF is configured with an advanced suite of physics parameterizations, including the Ferrier-Aligo microphysics scheme (Rogers et al., 2001), the Scale-Aware Simplified Arakawa-Schubert (SASAS) cumulus parameterization scheme (Arakawa & Schubert, 1974; Pan & Wu, 1995), and the RRTMG longwave and shortwave radiation schemes (Iacono et al., 2008; Mlawer et al., 1997). For more information about the HWRF system, readers are referred to the documentation (Biswas et al., 2018). We use the experimental Basin-scale HWRF (HWRF-B; Alaka et al., 2017, 2020; Zhang, Gopalakrishnan, et al., 2016; Zhang, Minamide, & Clothiaux, 2016) developed under the HFIP. HWRF-B has shown forecast improvement over the operational HWRF (Alaka et al., 2022). The HWRF-B configuration is nearly identical to that in the operational HWRF, except that HWRF-B uses storm-following nests for several TCs per model integration and has an outermost domain that does not move. Conversely, the operational HWRF has storm-following nested domains for only one TC per model integration and its outermost domain is relocated for each forecast.

In this study, we evaluate the retrospective HWRF-B simulations from 2018, which includes a total of 15 TCs from the North Atlantic and 22 TCs from eastern North Pacific (Table S1 in Supporting Information S1). Each simulation cycle had a length of 126 hr and simulations were produced every 6 hours. In total, 499 HWRF-B simulation cycles from 25 May to 31 October 2018 were utilized in this study. We only adopt the radiative heating fields at the 6-hr lead time in every simulation cycle to minimize the possible influence of model error at longer forecasting lead times. HWRF-B output was interpolated to one-degree resolution to match CERES data. We evaluate the current TC intensity and 24-hr intensity change in HWRF-B at 6-hr lead times and corresponding IBTrACS metrics (Figure S1 in Supporting Information S1). The mean intensity error at 6-hr lead time in the HWRF-B simulations is −1.17 kt with the root-mean-square error of 9.21 kt. The mean error of 24-hr intensity difference between 6-hr and 30-hr lead time is ∼0.4 kt with the root mean square error of 13.96 kt.

2.4. Longwave Radiative Fluxes

Previous modeling studies have demonstrated the importance of radiative fluxes to TC intensification. We only consider the longwave fluxes here, as the atmosphere is relatively transparent to shortwave radiation. Following Wu, Soden, and Nolan (2021) and Wu, Soden, Miyamoto, et al. (2021), we compute the vertical convergence of atmospheric longwave radiation (ALWC), which is:

$$\mathrm{ALWC} = \left(-\mathrm{LW_{up}}\right)_{\mathrm{TOA}} - \left(\mathrm{LW_{down}} - \mathrm{LW_{up}}\right)_{\mathrm{SFC}} \quad (1)$$

$\mathrm{LW_{up}}$ and $\mathrm{LW_{down}}$ are upward and downward longwave radiation, with the value of $\mathrm{LW_{up}}$ and $\mathrm{LW_{down}}$ being positive in the equation. The subscripts of TOA and SFC represent that variable is at the top-of-atmosphere and surface, respectively.

We also define ΔALWC as the difference in ALWC between HWRF simulations and CERES measurements. ΔALWC is defined as:

$$\Delta\mathrm{ALWC} = \mathrm{ALWC_{HWRF}} - \mathrm{ALWC_{CERES}} \quad (2)$$

The subscripts HWRF and CERES represent the data sources.

3. Results

3.1. Signals of TC Intensification in Satellite Measurements and HWRF

Composites of ALWC from CERES measurements are created to examine the relationship between ALWC and TC intensification. ALWC is composited separately for intensifying and weakening TCs and stratified into three

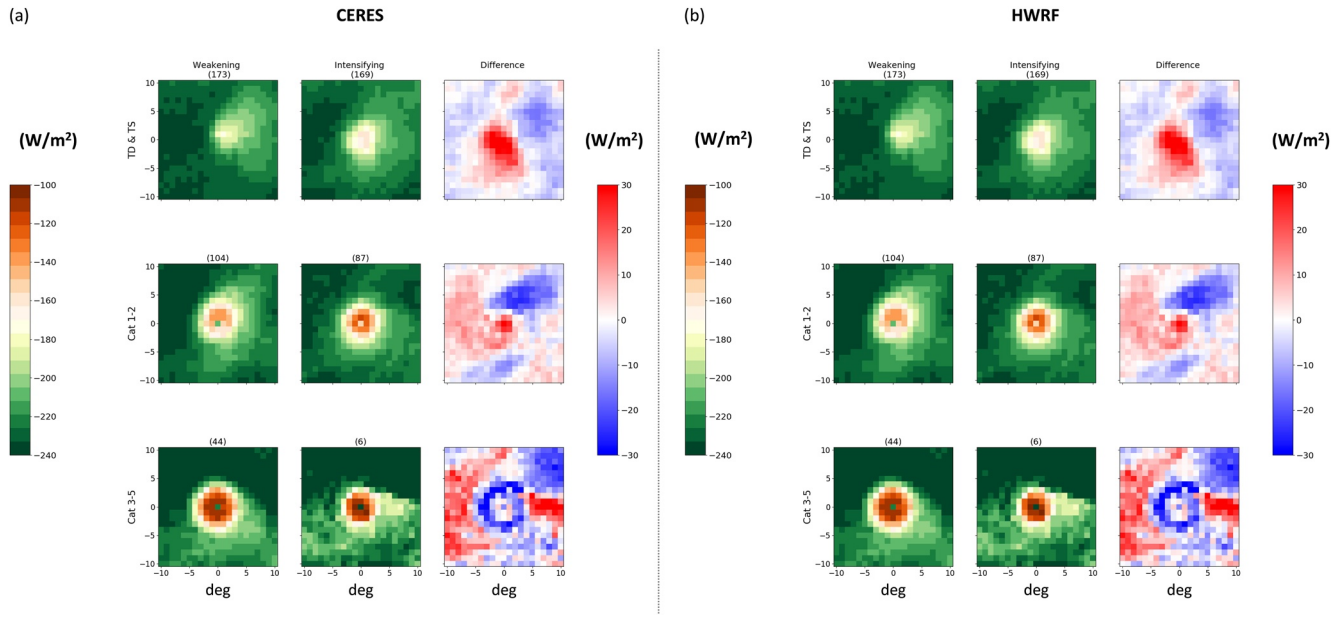

Figure 1. Storm-centered composites of ALWC from (a) CERES measurements and (b) HWRF simulations for TCs that weaken in the subsequent 24-hr period (left column), TCs that intensify in the subsequent 24-hr period (middle column), and intensifying TCs minus weakeningTCs (right column) in W/m^2. For CERES and HWRF, three rows from top to bottom are for different intensity categories: TD&TS, Cat 1–2, and Cat 3–5. For the left and middle columns, the number of cases in each composite is printed above the panel. Shadings are ALWC in W/m^2. The *x*- and *y*-axis are latitude and longitude in degrees relative to the TC center.

intensity categories based on its initial intensity classification. For both intensifying and weakening TCs, ALWC in the TC area (which tend to be covered by convective and stratiform clouds) is of ∼60–100 W/m^2 higher than that in the environment (Figure 1a). The reason for stronger ALWC in the TC area is mainly due to the thick layer of high clouds in the TC, which substantially reduces the energy loss to space from outgoing longwave radiation. The difference in ALWC between intensifying and weakening TCs (Figure 1a) is computed to examine how the distribution of ALWC affects TC intensification. For both TD/TS and category 1-2 storms, intensifying TCs have stronger ALWC of about 9 W/m^2 within 5-degree longitude/latitude and weaker ALWC in its environment, compared to weakening TCs. The 95% statistical significance level is reached for the area with the difference in ALWC greater than 10 W/m^2. For category 3–5, the difference between the TC area and its environment is not as clear as other intensity categories, implying that longwave radiative heating may be less effective to modulate strong TCs. This is to be expected given the greater contributions of latent heat release to the diabatic heating rates in strong TCs. The greater ALWC within the TC area in intensifying TCs can induce a large-scale transverse circulation, providing an upgradient transport of energy into TCs and accelerating the intensification processes (Ruppert et al., 2020). This greater ALWC signal in intensifying TCs is in agreement with recent modeling studies, which suggested that stronger cloud radiative heating in the precipitating area is a key to facilitate the development of TCs (Bretherton et al., 2005; Bu et al., 2014; Carstens & Wing, 2020; Muller & Romps, 2018; Smith et al., 2020; Wing et al., 2016; Wu, Soden, Miyamoto et al., 2021; Wu, Soden, Nolen 2021).

We repeat the same analyses for HWRF simulations, creating composites of ALWC, to examine the ability of the model to reproduce the observed radiative fluxes. The distribution of ALWC is similar to that in CERES measurements: ALWC in the TC area is ∼60 W/m^2 higher than that in its environment (Figure 1b). The average magnitude of ALWC in HWRF is ∼20 W/m^2 less than that in CERES measurements, with a slightly greater difference around the TC center. We also subtract composites of ALWC for weakening TCs from that for intensifying TCs to examine whether HWRF captures the observed relationship between ALWC and TC intensification. The signal of TC intensification in HWRF is consistent with that in CERES measurements: the TC area has positive differences, while the environment demonstrates a negative to small positive differences. In HWRF, an eye feature was clearly visible in hurricane composites for both weakening and intensifying cases even after the model data had been degraded to 1°, evidence that simulated eyes in HWRF are generally larger than observed (e.g., Otkin et al., 2017). Overall, HWRF successfully captures the pattern of ALWC shown in CERES measurements, though the magnitude of ALWC in HWRF is on average about 20 W/m^2 less than that observed.

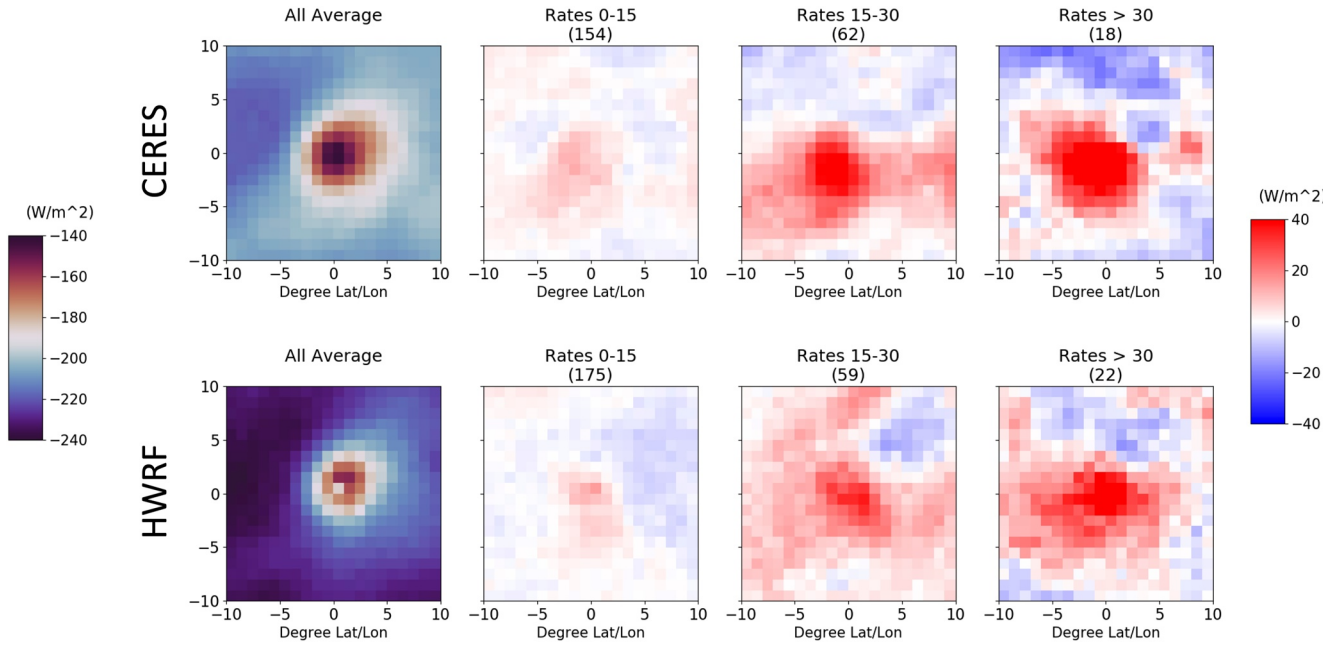

Figure 2. Storm-centered composites of ALWC from CERES measurements (top row) and HWRF simulations (bottom row). The left column, (a, e), depicts the mean ALWC for all TCs with a maximum intensity below 100 kt. The three rightmost columns show the difference in ALWC relative to (a, e) for three bins of 24-hr TC intensity change: (b, f) 0–15 kt, (c, g) 15–30 kt, and (d, h) >30 kt. The *x*-axis and *y*-axis are degrees in latitude and longitude relative to the TC center.

We further examine how the rate of TC intensification is related to the distribution of ALWC in both HWRF simulations and CERES measurements. To do this, the ALWC composites are created for three groups based on the 24-hr intensity change: 0–15 kt, 15–30 kt, and >30 kt (Figure 2). For reference, we also compute mean ALWC for all TCs with the intensity below 100 kt, as intensification in strong TCs is typically less affected by radiative heating than in weak TCs (see Figure 1). For both HWRF simulations and CERES measurements, the composite for all TCs demonstrates a similar ALWC, with greater ALWC in the TC area and lower values of ALWC in the environment. In terms of the relationship of ALWC with intensification rates, ALWC within the TC area becomes stronger as the intensification rate increases. This relationship is consistent between HWRF simulations and CERES measurements. It is worth noting that ALWC at the initial time can potentially be used to predict rapid intensification (change of 30+ kt in 24 hr; RI) in the HWRF forecast. For example, the area covered by ALWC greater than 40 Wm^{-2} is certainly larger for RI rate (Figure 2h) than for weaker intensification rates (Figures 2f and 2g). Interestingly, moderate intensification rates (15–30 kt per 24 hr) have a maximum ALWC greater than 40 Wm^{-2} (Figure 2g), but over a smaller area than RI rates. The results suggest that TCs with faster intensification rates tend to have a greater ALWC within the precipitating area as well as a stronger ALWC gradient between TC area and its environment. HWRF simulations reasonably replicate this observed relationship found in CERES measurements.

3.2. Impacts of Radiation on the Prediction Skills of TC Intensification

As HWRF has demonstrated its ability to reproduce the signal of TC intensification in ALWC, we extend our analysis to examine how the prediction skill of TC intensification is related to the model's performance in capturing the observed radiative fluxes. As radiative heating is demonstrated to be not as influential for intensity change in strong TCs (see Figure 1), the following analysis excludes Cat 3–5 TCs. We create the composites of ALWC for HWRF simulations that correctly predict the sign of 24-hr intensity change and for those that fail to (Figure 3). In the group associated with the correct prediction, the difference in ALWC composites between intensifying and weakening TCs is similar to that in CERES measurements: intensifying TCs have stronger ALWC within the TC core and weaker ALWC in the environment (Figures 3a and 3b). Conversely, the group associated with the incorrect prediction (Figures 3c and 3d) demonstrates the opposite pattern to that in CERES measurements. That is, the simulated ALWC within the convective area for TCs that incorrectly intensify is weaker compared to that for TCs that incorrectly weaken in the following 24 hr. The ALWC signal of TC intensification from the correct

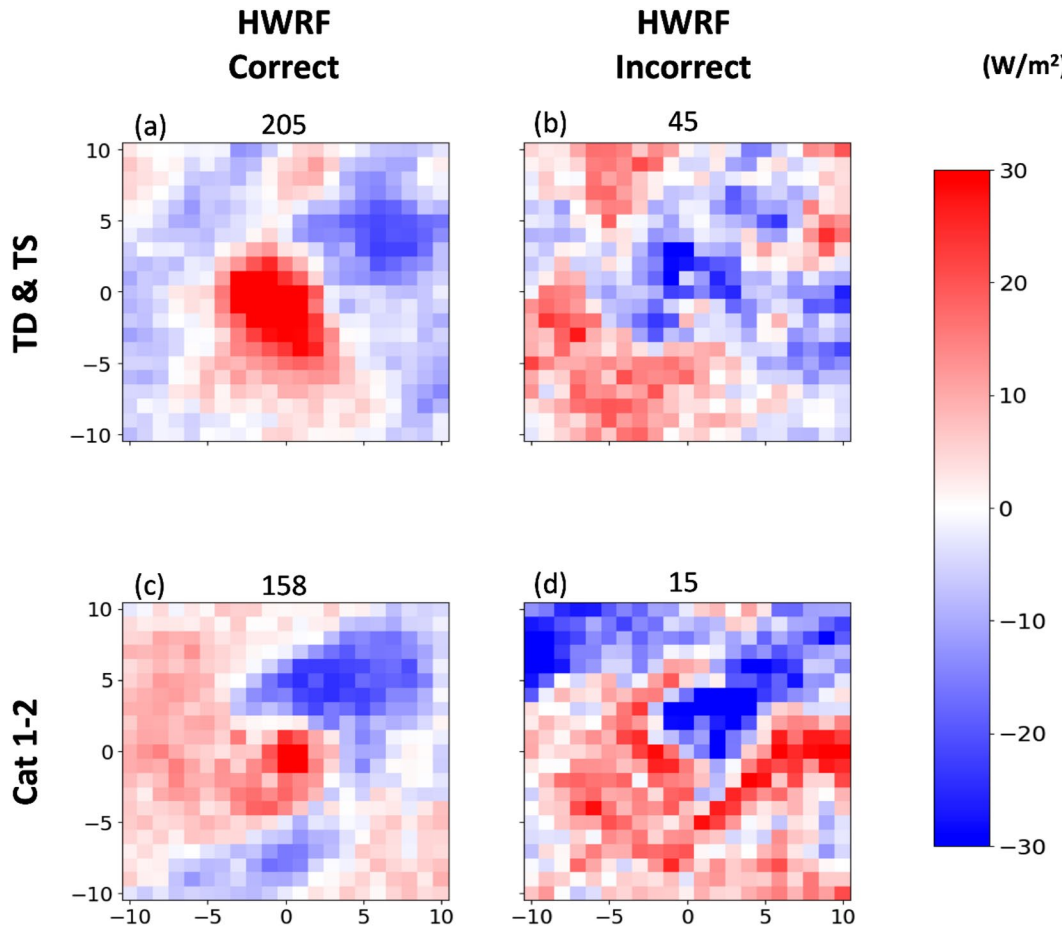

Figure 3. Storm-centered composites of the difference in the HWRF-simulated ALWC between TCs that will intensify and weaken during the following 24 hr. The left column is Intensity change events that are correctly predicted, and the right column is intensity change events that are incorrectly predicted. The two rows from top to bottom are for different 6-hr HWRF forecast intensity categories: (a, c) TD and TS, (b, d) Cat 1–2. The *x*-axis and *y*-axis are degrees in latitude and longitude relative to the TC center.

predictions agrees with what the observational metrics demonstrated and previous modeling studies suggested (Carstens & Wing, 2020; Muller & Romps, 2018; Smith et al., 2020; Wu, Soden, Miyamoto et al., 2021; Wu, Soden, Nolen 2021).

To quantitatively estimate the effect of the simulated radiative heating on the prediction skill of TC intensification, we examine how the performance of the intensity prediction (ΔV_t) is related to the difference in ALWC between HWRF and CERES (ΔALWC). We hypothesize that greater ΔALWC gradient between TC and environment corresponds to greater ΔV_t, as a strong ALWC gradient implies faster intensification or slower weakening. Therefore, the azimuthal average of ΔALWC, which is defined as the difference in ALWC between HWRF and CERES, is calculated for every storm from their TC center to the radial distance of 1,000 km. We separate the HWRF simulations into different groups based on ΔV_t, the deviation of simulated 24-hr intensity change from that in the IBTrACS.

$$\Delta V_t = (V_{24h} - V_{current})_{HWRF} - (V_{24h} - V_{current})_{BEST} \quad (3)$$

The subscripts HWRF and BEST represent TC intensity associated with HWRF simulations and IBTrACS, respectively. $V_{current}$ is current TC intensity and V_{24h} is TC intensity 24 hr from the current time. ΔALWC composites are created for the three groups based on ΔV_t: 0–10 kt, 10–20 kt, and 20–30 kt. Smaller ΔV_t, means better prediction skill. Similar to previous analysis, we also calculate mean ΔALWC for all TCs with the intensity below 100 kt for the reference.

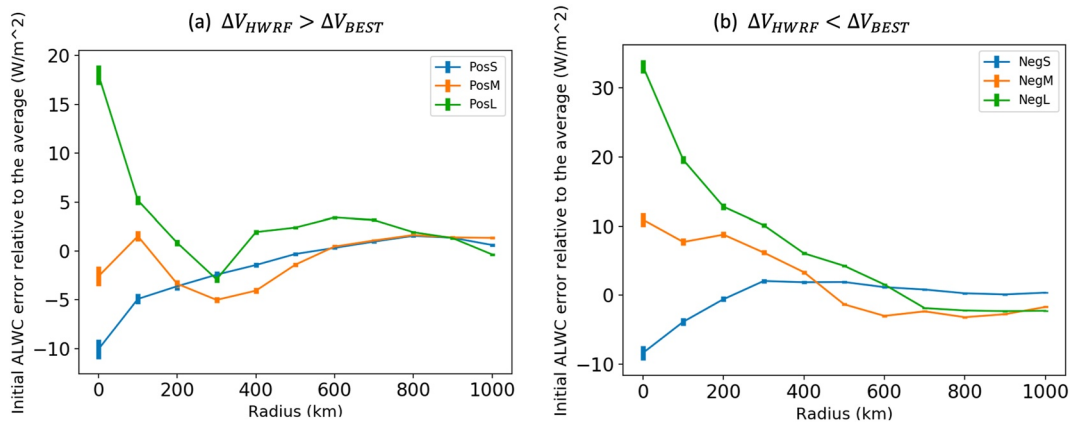

Figure 4. Storm-centered composites of azimuthal mean ΔALWC relative to the average ΔALWC of all selected storms for: (a) intensification rates in HWRF greater than BEST ($\Delta V_t > 0$), and (b) intensification rates in HWRF less than BEST ($\Delta V_t < 0$). The *x*-axis is radius to the TC center in km, and the *y*-axis is the initial ALWC error relative to the average in Wm^{-2}. Different line colors represent different magnitudes of ΔV_t in each panel. In (a), PosS (blue) represents 0 kt < $\Delta V_t \leq$ 10 kt, PosM (orange) represents 10 kt < $\Delta V_t \leq$ 20 kt, and PosL (green) represents 20 kt < $\Delta V_t \leq$ 30 kt. In (b), NegS (blue) represents 0 kt > $\Delta V_t \geq -10$ kt, NegM (orange) represents −10 kt > $\Delta V_t \geq -20$ kt, and NegL (green) represents −20 kt < $\Delta V_t \geq -30$ kt. Error bars represent standard error.

Considering positive ΔV_t, in which HWRF storms intensify faster or weaken slower than those in BEST, ΔALWC within 200 km of the TC center becomes greater as ΔV_t increases, suggesting that HWRF simulations with higher-than-expected ALWC tend to overestimate TC intensification rates (Figure 4a). ALWC error dips at around 200 km. This dip may imply the occurrence of a moat region between the TC inner core and rainbands in HWRF simulations, as less cloud production leads to smaller ALWC. The result is consistent with our previous analysis that greater inner-core ALWC can accelerate TC intensification. Nevertheless, among all the groups of negative ΔV_t, in which storms in HWRF weakens faster or intensify slower than BEST, the group with most negative ΔV_t also have greater ΔALWC within 200 km, suggesting that storms with overestimated weakening rates or underestimated intensification rates in HWRF prediction often have stronger simulated inner-core ALWC (Figure 4b). The main reason for the larger ΔALWC in the faster-weakening/slower-intensifying group (i.e., simulated storms project slower intensification rates than observation) could be due to their stronger simulated initial TC intensity compared with observations. As we expect that overestimated intensification rates lead to larger ΔALWC, the simulated storms with a greater initial intensity than corresponding observations are also likely to produce higher ΔALWC. To better investigate whether a stronger initial intensity in HWRF is the reason for the larger ΔALWC, we perform a similar analysis but only include simulations with initial intensity error of less than 5 kts. However, the larger ΔALWC still occurs in the faster-weakening/slower-intensifying group, implying that the large negative ΔV_t might involve other factors in addition to just radiation, while better capturing the initial ALWC in HWRF can produce a better intensity forecast.

We also compute the absolute value of ΔALWC to quantify the model's performance to replicate radiative fluxes and compare between TCs with different ΔV_t. The mean absolute value of ΔALWC within 500 km of the TC center is calculated for four different magnitudes of the absolute value of ΔV_t, which are 0–10, 10–20, 20–30, 30–40 kt. Progressing from small to large absolute values of ΔV_t, the magnitude of absolute ΔALWC grows monotonically from 32.5 to ∼42.5 W/m^2 (Figure S2 in Supporting Information S1). The model's failure to capture the timing of RI or to falsely predict RI could be driving a larger ALWC error for a larger error in intensification rates in the group with ΔV_t greater than 30 kt. The results demonstrate that the accuracy of predicting TC intensification in HWRF is positively correlated with the performance of reproducing ALWC. In addition, the chances of HWRF failing to predict the sign of intensity change also increases along with the increase of absolute ΔALWC. These results suggest that the simulations that capture the observed distribution of ALWC are more likely to accurately predict TC intensity change, while those that are unable to reproduce the observed ALWC tend to fail in predicting TC intensity change.

The influence of radiative heating on the predictive skill shown here is consistent with previous predictability-related studies which suggested that strong large-scale influence can effectively enhance the predictability of TC intensity

(Finocchio & Majumdar, 2017; Zhang & Tao, 2013). The results shown above suggest that the performance of predicting TC intensity in HWRF may substantially depend on the model's ability to accurately simulate the observed ALWC.

4. Summary

This study explores how the model's ability to replicate the observed distribution of radiative heating affects the prediction of TC intensification in an operational hurricane forecasting model, HWRF. The contrast of radiative heating between the TC area and the environment has been shown to be a key factor in promoting the development of TCs. In both HWRF simulations and CERES measurements, intensifying TCs on average have stronger atmospheric longwave radiation (ALWC) than weakening TCs within the TC area, while in the environment, their ALWC difference varies from negative to small positive values. Furthermore, both CERES measurements and HWRF simulations demonstrate that TCs with stronger ALWC tends to show a larger subsequent increase in TC intensity, and the HWRF also captures the ALWC gradient shown in rapidly intensifying TCs.

We further show that storms tend to have a better forecast of their subsequent 24-hr intensification change when the model better captures a spatial distribution of longwave heating. HWRF simulations that correctly predict 24-hr intensification change can reproduce the observed signal of TC intensification in ALWC, that is, stronger inner core ALWC for TCs that correctly intensify, while those that fail to capture 24-hr intensity change demonstrate the opposite relationship. In addition, simulations with better performance in predicting 24-hr intensity change produce smaller errors in ALWC, compared to those with mediocre performance. Failure to capture the timing of RI or false prediction of RI results in larger ALWC errors. The increase in intensity forecasting error along with greater error in radiative heating highlights the importance of correctly simulating radiative heating to TC predictions in numerical models.

In conclusion, this study demonstrates the close relationship between the numerical model prediction of TC intensification and the model's ability to replicate the ALWC in HWRF. The results suggested that ALWC could be used as guidance for the accuracy of intensification forecasts. If the model ALWC pattern at the initialization time matches that in observations, then a forecaster may have higher confidence in that HWRF forecast. It is also consistent with recent modeling studies which assimilated all-sky radiance from microwave satellite measurements to improve the performance of model simulations (Minamide & Zhang, 2018; Zhang, Gopalakrishnan, 2016; Zhang, Minamide et al., 2016; Zhang, Sieron, et al., 2021; Zhang, Soden, et al., 2021). Overall, this study supports previous modeling and observational studies which suggested that radiative heating plays a critical role in bolstering TC intensification. More analyses are required to explore the possible physical pathway for radiative heating to modulate TC development and assess the potential utility of observational radiative fluxes in hurricane prediction.

Data Availability Statement

CERES data were downloaded directly from CERES Data Product on NOAA website (https://ceres.larc.nasa.gov/data/). IBTrACS can be downloaded from the NOAA website (https://doi.org/10.25921/82ty-9e16) The HWRF-B forecast data used in this study can be downloaded from the University of Miami Library (https://doi.org/10.17604/2h87-n675).

Acknowledgments
The authors thank the Center for Computational Science at the University of Miami and the NOAA Environmental Security Computing Center High Performance Storage System provide computational resources for the analysis. This research was partially supported by NASA Awards 80NSSC18K1032 and 80NSSC23K0115.

References

Alaka, G. J., Jr., Sheinin, D., Thomas, B., Gramer, L., Zhang, Z., Liu, B., et al. (2020). A hydrodynamical atmosphere/ocean coupled modeling system for multiple tropical cyclones. *Atmosphere*, *11*(8), 869. https://doi.org/10.3390/atmos11080869

Alaka, G. J., Jr., Zhang, X., & Gopalakrishnan, S. G. (2022). High-definition hurricanes: Improving forecasts with storm-following nests. *Bulletin America Meteorology Social*, *103*(3), E680–E703. https://doi.org/10.1175/bams-d-20-0134.1

Alaka, G. J., Jr., Zhang, X., Gopalakrishnan, S. G., Goldenberg, S. B., & Marks, F. D. (2017). Performance of Basin-scale HWRF tropical cyclone track forecasts. *Weather and Forecasting*, *32*(3), 1253–1271. https://doi.org/10.1175/waf-d-16-0150.1

Arakawa, A., & Schubert, W. H. (1974). Interaction of a cumulus cloud ensemble with the large-scale environment, part I. *Journal of the Atmospheric Sciences*, *31*(3), 674–701. https://doi.org/10.1175/1520-0469(1974)031<0674:ioacce>2.0.co;2

Atlas, R., Tallapragada, V., & Gopalakrishnan, S. (2015). Advances in tropical cyclone intensity forecasts. *Marine Technology Society Journal*, *49*(6), 149–160. https://doi.org/10.4031/mtsj.49.6.2

Bao, J.-W., Gopalakrishnan, S., Michelson, S., Marks, F., & Montgomery, M. T. (2012). Impact of physics representations in the HWRFX on simulated hurricane structure and pressure–wind relationships. *Monthly Weather Review*, *140*(10), 3278–3299. https://doi.org/10.1175/mwr-d-11-00332.1

Biswas, M. K., Carson, L., Newman, K., Stark, D., Kalina, E., Grell, E., & Frimel, J. (2018). *Community HWRF users' guide v4. 0a*. NCAR.
Bretherton, C. S., Blossey, P. N., & Khairoutdinov, M. (2005). An energy-balance analysis of deep convective self-aggregation above uniform SST. *Journal of the Atmospheric Sciences*, *62*(12), 4273–4292. https://doi.org/10.1175/jas3614.1
Bu, Y. P., Fovell, R. G., & Corbosiero, K. L. (2014). Influence of cloud–radiative forcing on tropical cyclone structure. *Journal of the Atmospheric Sciences*, *71*(5), 1644–1662. https://doi.org/10.1175/jas-d-13-0265.1
Carstens, J. D., & Wing, A. A. (2020). Tropical cyclogenesis from self-aggregated convection in numerical simulations of rotating radiative-convective equilibrium. *Journal of Advances in Modeling Earth Systems*, *12*(5), e2019MS002020. https://doi.org/10.1029/2019ms002020
DeMaria, M., Sampson, C. R., Knaff, J. A., & Musgrave, K. D. (2014). Is tropical cyclone intensity guidance improving? *Bulletin of the American Meteorological Society*, *95*(3), 387–398. https://doi.org/10.1175/bams-d-12-00240.1
Doelling, D. R., Loeb, N. G., Keyes, D. F., Nordeen, M. L., Morstad, D., Nguyen, C., et al. (2013). Geostationary enhanced temporal interpolation for CERES flux products. *Journal of Atmospheric and Oceanic Technology*, *30*(6), 1072–1090. https://doi.org/10.1175/jtech-d-12-00136.1
Fermepin, S., & Bony, S. (2014). Influence of low-cloud radiative effects on tropical circulation and precipitation. *Journal of Advances in Modeling Earth Systems*, *6*(3), 513–526. https://doi.org/10.1002/2013ms000288
Finocchio, P. M., & Majumdar, S. J. (2017). The predictability of idealized tropical cyclones in environments with time-varying vertical wind shear. *Journal of Advances in Modeling Earth Systems*, *9*(8), 2836–2862. https://doi.org/10.1002/2017ms001168
Fovell, R. G., Bu, Y. P., Corbosiero, K. L., Tung, W.-W., Cao, Y., Kuo, H.-C., et al. (2016). Influence of cloud microphysics and radiation on tropical cyclone structure and motion. *Meteorological Monographs*, *56*, 11–1. https://doi.org/10.1175/amsmonographs-d-15-0006.1
Fueglistaler, S. (2019). Observational evidence for two modes of coupling between sea surface temperatures, tropospheric temperature profile, and shortwave cloud radiative effect in the tropics. *Geophysical Research Letters*, *46*(16), 9890–9898. https://doi.org/10.1029/2019gl083990
Gall, R., Franklin, J., Marks, F., Rappaport, E. N., & Toepfer, F. (2013). The hurricane forecast improvement project. *Bulletin of the American Meteorological Society*, *94*(3), 329–343. https://doi.org/10.1175/bams-d-12-00071.1
Gopalakrishnan, S., Upadhayay, S., Jung, Y., & Coauthors (2021). 2020 HFIP R&D activities summary: Recent results and operational implementation.
Gopalakrishnan, S. G., Goldenberg, S., Quirino, T., Zhang, X., Marks, F., Jr., Yeh, K.-S., et al. (2012). Toward improving high-resolution numerical hurricane forecasting: Influence of model horizontal grid resolution, initialization, and physics. *Weather and Forecasting*, *27*(3), 647–666. https://doi.org/10.1175/waf-d-11-00055.1
Gopalakrishnan, S. G., Marks, F., Jr., Zhang, J. A., Zhang, X., Bao, J.-W., & Tallapragada, V. (2013). A study of the impacts of vertical diffusion on the structure and intensity of the tropical cyclones using the high-resolution HWRF system. *Journal of the Atmospheric Sciences*, *70*(2), 524–541. https://doi.org/10.1175/jas-d-11-0340.1
Gopalakrishnan, S. G., Marks, F., Jr., Zhang, X., Bao, J.-W., Yeh, K.-S., & Atlas, R. (2011). The experimental HWRF system: A study on the influence of horizontal resolution on the structure and intensity changes in tropical cyclones using an idealized framework. *Monthly Weather Review*, *139*(6), 1762–1784. https://doi.org/10.1175/2010mwr3535.1
Hakim, G. J. (2013). The variability and predictability of axisymmetric hurricanes in statistical equilibrium. *Journal of the Atmospheric Sciences*, *70*(4), 993–1005. https://doi.org/10.1175/jas-d-12-0188.1
Iacono, M. J., Delamere, J. S., Mlawer, E. J., Shephard, M. W., Clough, S. A., & Collins, W. D. (2008). Radiative forcing by long-lived greenhouse gases: Calculations with the aer radiative transfer models. *Journal of Geophysical Research*, *113*(D13), D13103. https://doi.org/10.1029/2008jd009944
Judt, F., & Chen, S. S. (2016). Predictability and dynamics of tropical cyclone rapid intensification deduced from high-resolution stochastic ensembles. *Monthly Weather Review*, *144*(11), 4395–4420. https://doi.org/10.1175/mwr-d-15-0413.1
Knapp, K. R., Kruk, M. C., Levinson, D. H., Diamond, H. J., & Neumann, C. J. (2010). The international best track archive for climate stewardship (IBTRACS) unifying tropical cyclone data. *Bulletin of the American Meteorological Society*, *91*(3), 363–376. https://doi.org/10.1175/2009bams2755.1
Lewis, W. E., Velden, C. S., & Stettner, D. (2020). Strategies for assimilating high-density atmospheric motion vectors into a regional tropical cyclone forecast model (HWRF). *Atmosphere*, *11*(6), 673. https://doi.org/10.3390/atmos11060673
Loeb, N. G., Wang, H., Allan, R. P., Armour, K., Cole, J. N. S., Andrews, T., et al. (2020). New generation of climate models track recent unprecedented changes in Earth's radiation budget observed by CERES. *Geophysical Research Letters*, *47*(5), e2019GL086. https://doi.org/10.1029/2019gl086705
Mehra, A., Tallapragada, V., Zhang, Z., Liu, B., Zhu, L., Wang, W., & Kim, H.-S. (2018). Advancing the state of the art in operational tropical cyclone forecasting at NCEP. *Tropical Cyclone Research and Review*, *7*(1), 51–56.
Melhauser, C., & Zhang, F. (2014). Diurnal radiation cycle impact on the pregenesis environment of hurricane KARL (2010). *Journal of the Atmospheric Sciences*, *71*(4), 1241–1259. https://doi.org/10.1175/jas-d-13-0116.1
Minamide, M., & Zhang, F. (2018). Assimilation of all-sky infrared radiances from Himawari-8 and impacts of moisture and hydrometer initialization on convection-permitting tropical cyclone prediction. *Monthly Weather Review*, *146*(10), 3241–3258. https://doi.org/10.1175/mwr-d-17-0367.1
Mlawer, E. J., Taubman, S. J., Brown, P. D., Iacono, M. J., & Clough, S. A. (1997). Radiative transfer for inhomogeneous atmospheres: RRTM, a validated correlated-k model for the longwave. *Journal of Geophysical Research*, *102*(D14), 16663–16682. https://doi.org/10.1029/97jd00237
Muller, C. J., & Held, I. M. (2012). Detailed investigation of the self-aggregation of convection in cloud-resolving simulations. *Journal of the Atmospheric Sciences*, *69*(8), 2551–2565. https://doi.org/10.1175/jas-d-11-0257.1
Muller, C. J., & Romps, D. M. (2018). Acceleration of tropical cyclogenesis by self-aggregation feedbacks. *Proceedings of the National Academy of Sciences of the United States of America*, *115*(12), 2930–2935. https://doi.org/10.1073/pnas.1719967115
Otkin, J. A., Lewis, W. E., Lenzen, A. J., McNoldy, B. D., & Majumdar, S. J. (2017). Assessing the accuracy of the cloud and water vapor fields in the hurricane WRF (HWRF) model using satellite infrared brightness temperatures. *Monthly Weather Review*, *145*(5), 2027–2046. https://doi.org/10.1175/mwr-d-16-0354.1
Pan, H.-L., & Wu, W.-S. (1995). Implementing a Mass flux convection parameterization package for the NMC medium-range forecast model. NMC Office Note No. 409 1995 (p. 40). Retrieved from https://repository.library.noaa.gov/view/noaa/11429
Randall, D. A., Dazlich, D. A., & Corsetti, T. G. (1989). Interactions among radiation, convection, and large-scale dynamics in a general circulation model. *Journal of the Atmospheric Sciences*, *46*(13), 1943–1970. https://doi.org/10.1175/1520-0469(1989)046<1943:iarcal>2.0.co;2
Rogers, E., Black, T., Ferrier, B., Lin, Y., Parrish, D., & DiMego, G. (2001). Ncep meso eta analysis and forecast system: Increase in resolution, new cloud microphysics, modified precipitation assimilation, modified 3DVAR analysis. *NWS Technical Procedures Bulletin*, *488*, 1–15.
Ruppert, J. H., Jr., Wing, A. A., Tang, X., & Duran, E. L. (2020). The critical role of cloud–infrared radiation feedback in tropical cyclone development. *Proceedings of the National Academy of Sciences of the United States of America*, *117*(45), 27884–27892. https://doi.org/10.1073/pnas.2013584117

Sherwood, S. C., Ramanathan, V., Barnett, T. P., Tyree, M. K., & Roeckner, E. (1994). Response of an atmospheric general circulation model to radiative forcing of tropical clouds. *Journal of Geophysical Research*, *99*(D10), 20829–20845. https://doi.org/10.1029/94jd01632

Simon, A., Penny, A. B., DeMaria, M., Franklin, J. L., Pasch, R. J., Rappaport, E. N., & Zelinsky, D. A. (2018). A description of the real-time HFIP corrected consensus approach (HCCA) for tropical cyclone track and intensity guidance. *Weather and Forecasting*, *33*(1), 37–57. https://doi.org/10.1175/waf-d-17-0068.1

Smith, W. P., Nicholls, M. E., & Pielke, R. A., Sr. (2020). The role of radiation in accelerating tropical cyclogenesis in idealized simulations. *Journal of the Atmospheric Sciences*, *77*(4), 1261–1277. https://doi.org/10.1175/jas-d-19-0044.1

Tallapragada, V., Kieu, C., Kwon, Y., Trahan, S., Liu, Q., Zhang, Z., & Kwon, I.-H. (2014). Evaluation of storm structure from the operational HWRF during 2012 implementation. *Monthly Weather Review*, *142*(11), 4308–4325. https://doi.org/10.1175/mwr-d-13-00010.1

Wang, W., Sippel, J. A., Abarca, S., Zhu, L., Liu, B., Zhang, Z., et al. (2018). Improving NCEP HWRF simulations of surface wind and inflow angle in the eyewall area. *Weather and Forecasting*, *33*(3), 887–898. https://doi.org/10.1175/waf-d-17-0115.1

Wielicki, B. A., Barkstrom, B. R., Harrison, E. F., Lee, R. B., III, Smith, G. L., & Cooper, J. E. (1996). Clouds and the Earth's radiant energy system (CERES): An Earth observing system experiment. *Bulletin of the American Meteorological Society*, *77*(5), 853–868. https://doi.org/10.1175/1520-0477(1996)077<0853:catere>2.0.co;2

Wing, A. A., Camargo, S. J., & Sobel, A. H. (2016). Role of radiative–convective feedbacks in spontaneous tropical cyclogenesis in idealized numerical simulations. *Journal of the Atmospheric Sciences*, *73*(7), 2633–2642. https://doi.org/10.1175/jas-d-15-0380.1

Wing, A. A., & Emanuel, K. A. (2014). Physical mechanisms controlling self-aggregation of convection in idealized numerical modeling simulations. *Journal of Advances in Modeling Earth Systems*, *6*(1), 59–74. https://doi.org/10.1002/2013ms000269

Wu, S.-N., Soden, B., & Alaka, G., Jr. (2020). Ice water content as a precursor to tropical cyclone rapid intensification. *Geophysical Research Letters*, *47*(21), e2020GL089. https://doi.org/10.1029/2020gl089669

Wu, S.-N., Soden, B., & Nolan, D. (2021). Examining the role of cloud radiative interactions in tropical cyclone development using satellite measurements and WRF simulations. *Geophysical Research Letters*, *48*(15), e2021GL093. https://doi.org/10.1029/2021gl093259

Wu, S.-N., & Soden, B. J. (2017). Signatures of tropical cyclone intensification in satellite measurements of ice and liquid water content. *Monthly Weather Review*, *145*(10), 4081–4091. https://doi.org/10.1175/mwr-d-17-0046.1

Wu, S.-N., Soden, B. J., Miyamoto, Y., Nolan, D. S., & Buehler, S. A. (2021). Using satellite observations to evaluate the relationships between ice condensate, latent heat release, and tropical cyclone intensification in a mesoscale model. *Monthly Weather Review*, *149*(1), 113–129. https://doi.org/10.1175/mwr-d-19-0348.1

Zhang, B., Soden, B. J., Vecchi, G. A., & Yang, W. (2021). The role of radiative interactions in tropical cyclone development under realistic boundary conditions. *Journal of Climate*, *34*(6), 2079–2091. https://doi.org/10.1175/jcli-d-20-0574.1

Zhang, F., Minamide, M., & Clothiaux, E. E. (2016). Potential impacts of assimilating all-sky infrared satellite radiances from GOES-R on convection-permitting analysis and prediction of tropical cyclones. *Geophysical Research Letters*, *43*(6), 2954–2963. https://doi.org/10.1002/2016gl068468

Zhang, F., & Tao, D. (2013). Effects of vertical wind shear on the predictability of tropical cyclones. *Journal of the Atmospheric Sciences*, *70*(3), 975–983. https://doi.org/10.1175/jas-d-12-0133.1

Zhang, X., Gopalakrishnan, S. G., Trahan, S., Quirino, T. S., Liu, Q., Zhang, Z., et al. (2016). Representing multiple scales in the Hurricane Weather Research and Forecasting Modeling system: Design of multiple sets of movable multilevel nesting and the basin-scale HWRF forecast application. *Weather and Forecasting*, *31*(6), 2019–2034. https://doi.org/10.1175/WAF-D-16-0087.1

Zhang, Y., Sieron, S. B., Lu, Y., Chen, X., Nystrom, R. G., Minamide, M., et al. (2021). Ensemble-based assimilation of satellite all-sky microwave radiances improves intensity and rainfall predictions for hurricane Harvey (2017). *Geophysical Research Letters*, *48*(24), e2021GL096. https://doi.org/10.1029/2021GL096410